7(h). Mat-related features from the Terminal Ediacaran Nudaus Formation, Nama Group, Namibia

E. Bouougri and H. Porada

The Nama Group in central to southern Namibia (Fig. 7(h)-1A) represents the filling of a foreland basin related to the Neoproterozoic-Early Palaeozoic collision and uplift of the Damara and Gariep belts. The group is subdivided (from base to top) into the Kuibis, Schwarzrand and Fish River Subgroups (e.g., Germs, 1983; Gresse and Germs, 1993). During deposition of much of the earlier subgroups, the basin was divided by a flexural high (Osis ridge) into the southern Witputs and the northern Zaris sub-basins (Germs, 1983). Deformation of the Nama Group generally is weak but increases in the peripheries of the belts where open folds, slaty cleavage and minor thrusts occur. Based on palaeontological and radiometric data (Germs et al., 1986; Grotzinger et al., 1995, 2000), deposition of the Kuibis and most of the Schwarzrand Subgroups occurred in the Ediacaran. The studied outcrops belong to the Niederhagen and Vingerbreek members (Nudaus Formation) of the lower Schwarzrand Subgroup (Fig. 7(h)-1B). The age of the Nudaus Formation is between ca. 548 and 545 Ma, according to U-Pb zircon dates from ash layers in the underlying Kuibis Subgroup and overlying Urusis Formation, respectively (Grotzinger et al., 1995). The members consist of shale, siltstone and sandstone, all deposited in tidal and low-energy shoreline depositional environments (Germs, 1983). The study area (Fig. 7(h)-1C), located in the northwestern part of the Zaris sub-basin, straddles the facies boundary of "mainly sandy tidal" and "muddy tidal without carbonate, some distal fluvial sediments" (Germs, 1983, p. 102). Sequence stratigraphic studies further south in the basin showed the Vingerbreek member to include shallowing-upward cycles of nearshore to mid-shelf shale, siltstone and intercalated sandstone beds, deposited in a transgressive systems tract (Saylor et al., 1995).

Occurrences of mat-related structures described here from the Nudaus Formation, come mainly from the lowermost part of the Vingerbreek Member, exposed near Haruchas homestead (Figs.7(h)-2A, -2E, -2H, 7(h)-3 and 7(h)-4). At this locality, a section of about 46 m thickness contains various microbial mat-related structures (Porada and Bouougri, 2006) which complement 'wrinkle structures' described by Noffke et al. (2002) from the upper part of the member, further to the SW near the Sattelberg mountain. The section consists mainly of thinly bedded, fine-grained siliciclastic deposits bounded by major sandstone bodies below and above. The section starts with a sheet-like sandstone bed, 0.8 m thick, with large-scale hummocky cross- stratification (HCS) reflecting a depositional environment influenced by storms. Overlying this is a heterolithic succession, about 43 m thick, of laminated siltstone/argillite with few interbedded sandstone layers. Within this interval, the biolaminite lithofacies constitutes the main component and alternates with minor laminated siltstone-mudstone lithofacies. Intercalated sandstone beds and bodies originated from intermittent storm-induced oscillatory currents or represent small-scale tidal channel-fills cutting into the heterolithic deposits.The section is capped by a 3 m sandstone body that is interpreted as fluvial channel deposits, consisting of coarse- to medium-grained cross-bedded and lenticular sandstone with lenses of conglomerate,

which also exhibits erosional scouring as indicated by gutter casts, flute casts and the erosional base.

The biolaminite lithofacies is developed in metre-scale intervals, separated by centimetre-scale fine-grained sandstone beds, and consists of thinly interlaminated layers of siltstone and dark to black material of variable thickness and proportions. The silty laminae frequently exhibit wave ripple cross-lamination and small interference and oscillation ripples with sharp crests. The rippled surfaces are commonly draped by a dark and continuous film of mudstone.

The biolaminite lithofacies encompasses structures which record cyclic mat growth and destruction processes during biosedimentary accretion. Evidence of the participation of microbial mats that once colonized the sedimentary surfaces and contributed to the accretion of thick stacked layers of biolaminite include microscopic and macroscopic features like 'wavy-crinkly' lamination, isolated silt-sized grains enclosed in sericitic carbonaceous layers, 'elephant skin' textures, spindle-shaped and lenticular shrinkage cracks, lenticular cracks with upturned margins and subcircular cracks with upturned and curled margins (Figs.7(h)-2, 7(h)-3). The structures are developed on single and thin microbial mat layers or encompass stacks of biolaminites. Most diagnostic are networks of upturned to overturned crack margins (Fig.7(h)-3H; see also Fig.4(c)-6D, -6E) which are overlain by continuous, planar biolaminated deposits preserving the original sedimentation plane.

The sedimentary features of the heterolithic and biolaminated deposits collectively indicate sedimentation in a shallow, intertidal to lower supratidal environment characterized by periodic emergence and occasional high energy events such as storms or tidal floods. The vertical facies organization records an upward evolution from storm-dominated subtidal sand bar to fluvial deposits, and indicates progradational and shallowing-upward trends. In this scenario, the basal, HCS-bearing sandstone bed is considered to reflect a storm barrier or sand-shoal in a nearshore setting. Landwards, behind the barrier, low hydrodynamic energy combined with a low rate of sediment supply would have been expected, thus creating favourable conditions for microbial mat growth and biosedimentary accretion of biolaminites. Indeed, development of microbial mats is indicated by strong bioturbation by undermat miners (Fig.7(h)-4) just a few decimetres above the storm bar (cf. Aigner and Reineck, 1982). Microbial growth was occasionally interrupted by storms or high-energy tidal events resulting in the deposition of thicker sandy layers. One of them is extensively covered by *Kinneyia*-type wrinkle structures (Fig.7(h)-2H). Still further landwards, the peritidal deposits graded into fluvial sandy deposits, due to seaward progradation of a fluvial system onto the peritidal area.

Further structures of *Kinneyia*-type wrinkles are reported from the Niederhagen Member near Urikos homestead (Fig.7(h)-2G) and from the middle part of the Vingerbreek Member at Haruchas (7(h)-2F). In both cases, the structures occur at the tops of thickening- and shallowing-upward cycles, reflecting fluvial/storm influenced delta front-peritidal coastal/delta plain evolutions. As indicated by the thickness of the corresponding deposits, the coastal/delta plain settings formed only short time intervals within prograding cycles. The *Kinneyia* structures are developed on centimetre- to decimetre-thick sandstone layers of an intertidal 'coastal/delta plain'

setting, in which high-energy event sand layers are capped by low-energy laminated siltstone/mudstone. Only a few, centimetre-thick sandstone layers of the coastal/delta plain deposits preserve lenticular and tri-radiate shrinkage cracks similar to those of Fig. 7(h)-3E. The rarity of mat-related structures in such settings seems to be controlled by sedimentary dynamics. Within the cycles, short-time developments of peritidal coastal/delta plain environments appear to be related to rapid drowning and resulting increase in accommodation space, which inhibited widespread growth of microbial mats and accretion of thick biolaminites.
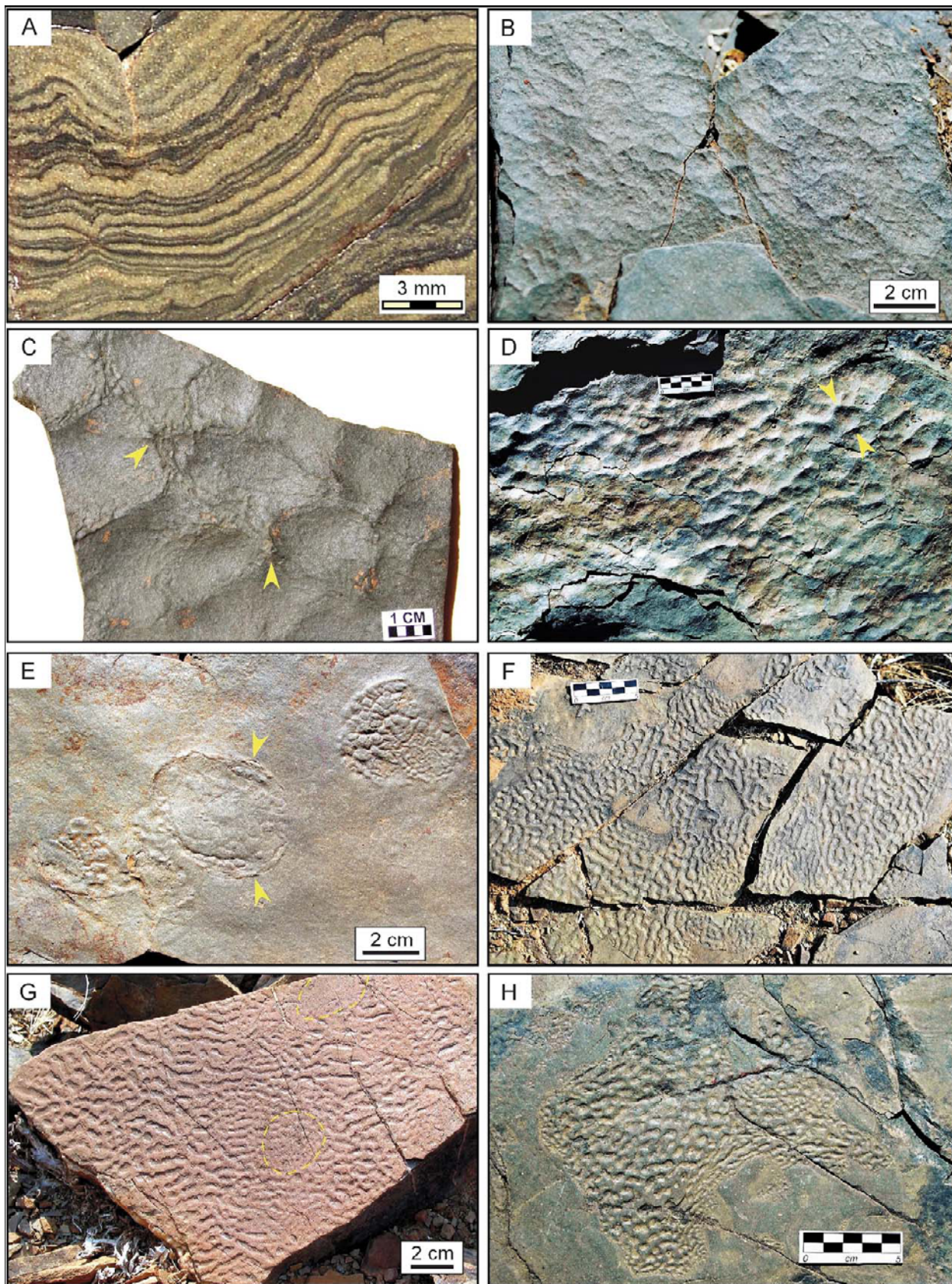
Figures
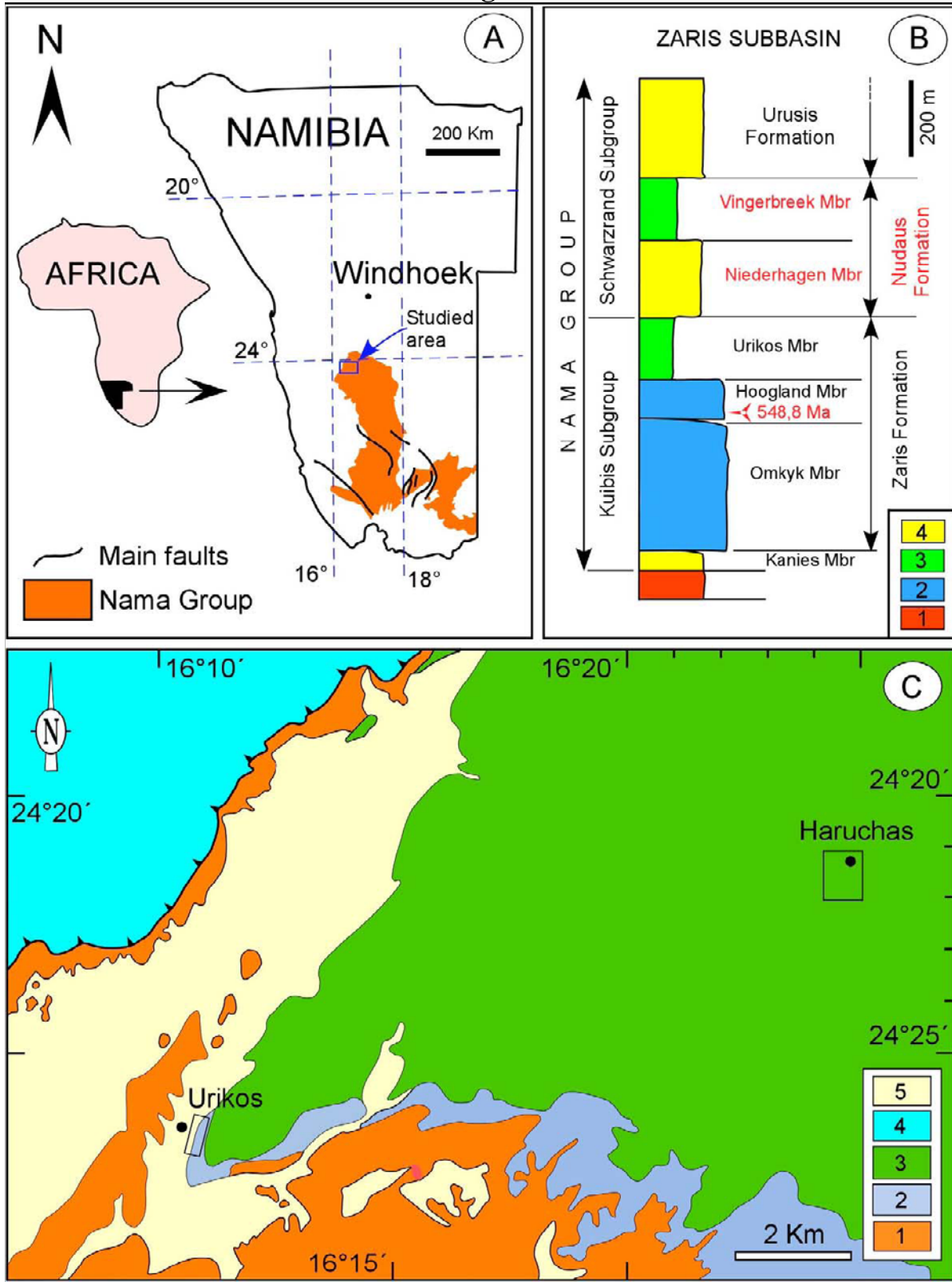
In: *Atlas of microbial mat features preserved within the clastic rock record*, Schieber, J., Bose, P.K., Eriksson, P.G., Banerjee, S., Sarkar, S., Altermann, W., and Catuneau, O., (Eds.)J. Schieber et al. (Eds.), Elsevier, p. 214-221. (2007)

Figure 7(h)-1: Location and stratigraphy of the Nama Group study area.
(A) Distribution of Nama Group deposits in central and southern Namibia and location of study area (simplified from Geological Map of Namibia). (B) Generalised lithostratigraphic column of part of the Nama Group in the study area of the Zaris Sub-basin (age data from Grotzinger et al., 1995). 1 – Basement, 2–4 – Dominant lithologies in Kuibis and Schwarzrand Subgroup: 2 – limestone, 3 – mudstone, 4 – sandstone. (C) Simplified geological map of the study area showing the localities of Haruchas and Urikos (from Geological Survey of Namibia, 1980, 1/250000 Geological series, Sheet 2416 Mariental). 1 – Kuibis Subgroup; 2, 3 – Schwarzrand Subgroup: 2 – Niederhagen Member, 3 – Vingerbreek Member; 4 – Naukluft nappe complex; 5 – Quaternary deposits.
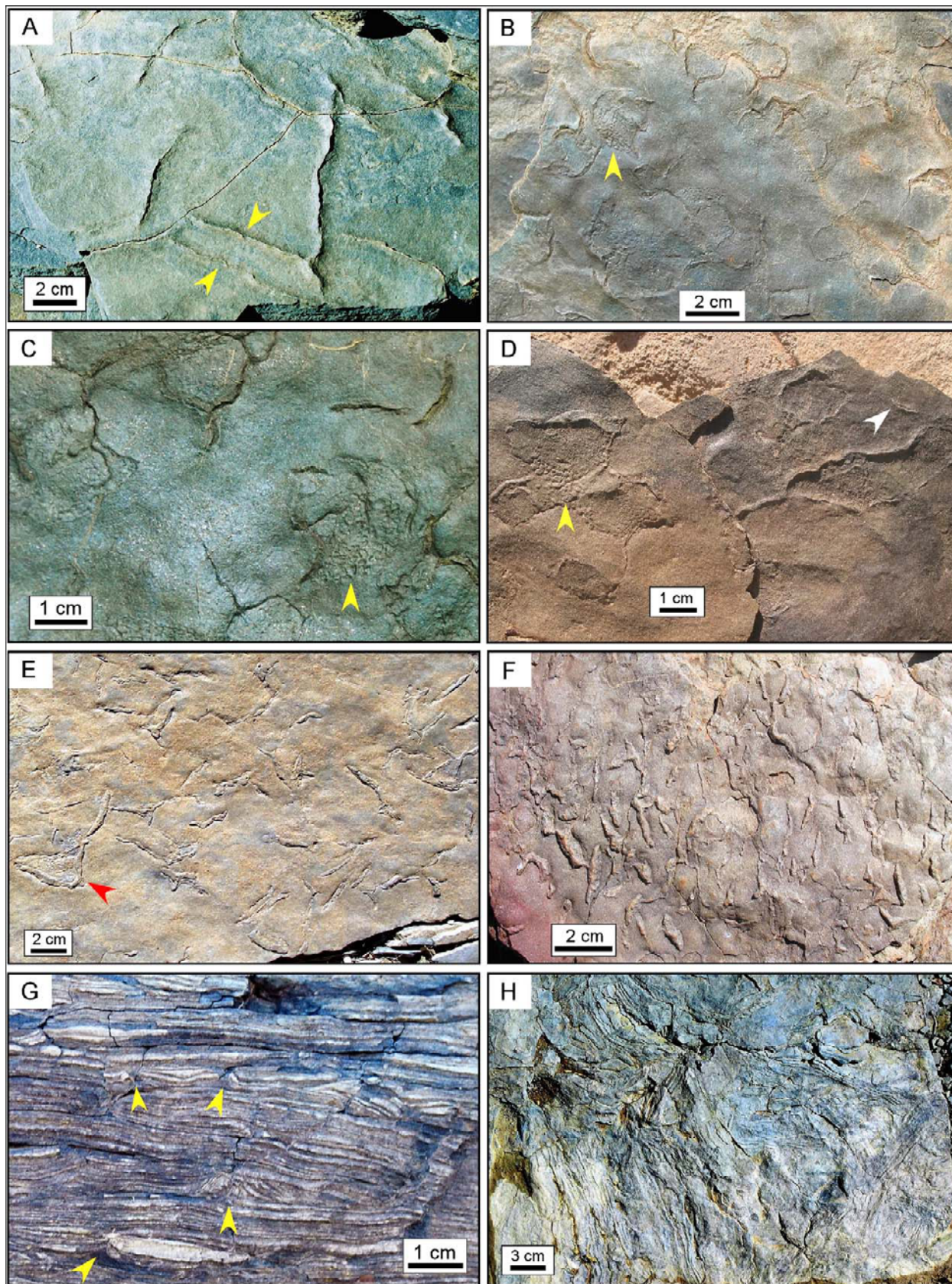
In: *Atlas of microbial mat features preserved within the clastic rock record*, Schieber, J., Bose, P.K., Eriksson, P.G., Banerjee, S., Sarkar, S., Altermann, W., and Catuneau, O., (Eds.)J. Schieber et al. (Eds.), Elsevier, p. 214-221. (2007)

Figure 7(h)-2: Growth, surface and subsurface structures: biolaminites (A), mat-growth and mat surface structures (B–E), subsurface *Kinneyia* structures (F–H).
(A) Polished section of biolaminite showing millimetre-scale alternation of dark microbial mat layers and light silt/sand-sized quartz layers. Thickness and proportions of the layers are variable. The dark microbial mat layers consist of sericite and relics of carbonaceous material and include isolated silt-sized grains and abundant muscovite flakes 'floating' in the sericitic groundmass. Such organic layers draping siltstone laminae may be reduced to a very thin veneer of a few μm in thickness. In the light layers, sediment grains frequently are surrounded by sericite, developing a 'coated grain fabric'. Locality: Vingerbreek Member, Farm Haruchas. Genesis: The millimetre-scale multilayered biolaminites result from the interplay of microbial mat growth and sediment deposition. The resulting bio-sedimentary lamination developed in a low-energy intertidal zone as indicated by associated sedimentary and other mat-related structures. Variations in thickness of microbial mat–siltstone doublets may have been controlled by tidal cycles, rate of sediment supply and frequency of high energy events. The process leading to biolaminites includes periods of non-deposition in which cyanobacteria produce and establish mat layers on a sediment surface, and periods of sedimentation in which the mat is covered by a thin layer of fine-grained sediment through which motile bacteria can move upwards to establish a new mat on top of this sediment (Gerdes et al., 2000a). Establishment of a new mat layer was usually achieved within several weeks of almost zero deposition, by motile bacterial taxa (e.g., *Microcoleus chthonoplasates, Lynbya aestuarii, Oscillatoria limosa*) or cell aggregates of them, which phototactically moved upwards from the buried mat and accumulated on the new surface (see Gerdes et al., 2000a; Gerdes and Klenke, 2003; also this volume: Chapter 2). (B) Upper bedding surface showing 'elephant skin' pattern consisting of narrow and sharp-crested ridges arranged in polygons with preferred orientation. In between the centimetre-scale sinuous ridges, a millimetre-scale reticulate pattern with polygonal network is developed. Locality: Vingerbreek Member, Farm Haruchas. (C) Close-up view of upper bedding surface showing 'reticulate pattern' of sharp-crested ridges in a centimetre-scale polygonal to almost hexagonal arrangement. A millimetre-scale reticulate structure is superposed on the large one, developed mainly along the higher parts of the troughs. Relics of tufts, up to 3 mm high (arrows), are preserved at junctional positions of the crests. The polygons are symmetric or elongate and are of varying diameter. Locality: Vingerbreek Member, Farm Haruchas. (D) Upper bedding surface exhibiting a network of discontinuous and sinuous sharp-crested ridges in a linear arrangement partly evolving into a polygonal pattern. The ridges follow continuously along the tops of the ripple crests but in a few cases may extend to the inter-crest zones. Length of crests may be up to 12 cm, whereas inter-crest distances are less than 4 cm. The crests may be symmetric or asymmetric in section (arrows). The sharp-crested 'rippled' surface is restricted to a 2 mm thick siltstone lens. Locality: Vingerbreek Member, Farm Haruchas. Scale is in cm. (E) Upper bedding surface with centimetre-scale subcircular structures. The structure in the centre preserves relics of a flattened sand margin (arrows) which corresponds to a curled crack margin related to desiccation of a thin microbial mat (see Figures 7(h)-3B to -3D). The structure in the upper right part of the photo displays a crinkly surface consisting of millimetre-scale round-crested to partly sharp-crested ridges separated by narrow troughs. Locality: Vingerbreek Member, Farm Haruchas. *Genesis of structures in Figures 7(h)-2B to -2E*: The structures in Figures 7(h)-2B, -2C are typical 'mat surface structures' resulting from reticulate growth patterns, called 'elephant-skin texture' in ancient deposits (Gehling, 1999). The structures associated with bedding surfaces of biolaminites illustrate the diversity in development and preservation of growth structures. Similar growth patterns have been described from modern tidal flats in southern Tunisia (e.g., Gerdes et al., 2000a) and attributed to vertical growth of cyanobacterial filaments (e.g., of *Microcoleus chthonoplastes*, *Lyngbya aestuarii*) forming tufts, pinnacles and ridges. The bedding surface characterised by sharp-crested linear to partly polygonal ridges (Figure 7(h)-3D) suggests a dominating linear growth pattern, which occasionally is also observed on the modern tidal flats of Southern Tunisia (see Figure 3(c)-3A). Linear growth patterns may be induced by a rippled sedimentary surface on which growth ridges preferably follow a ripple crest. Some linear growth patterns may present similarities with ridges resulting from slow downslope creeping of mat layers (G. Gerdes, personal comm., 2006). The structures seen in Figure 7(h)-2E are developed in subcircular openings of a mat with relics of a curled margin (see Figure 7(h)-3); they reflect surface or subsurface structures of a very thin mat which newly grew within the opening (see also Figure 7(h)-3B). (F) Upper bedding surface of 10 cm thick quartzite bed with well developed typical *Kinneyia* structure. The structure, occurring on a flat bedding surface, consists of irregular and sinuously curved crests, gently oversteepened and partly bifurcating. Crests are separated by subcircular to elongate curved inter-crest depressions and pits with an average diameter/width of 4–6 mm. Locality: Vingerbreek Member, Farm Haruchas (S 24◦22_37.5__, E 016◦22_42.4__). Scale in cm. (G) Upper bedding surface of 8 cm thick quartzite bed with typical *Kinneyia* structure.

The structure consists of long winding and flat-topped crests with a preferred orientation, and intervening pits and troughs. The regularly distributed pits and depressions are elongate (1 to 3 cm in length) and sinuously to gently curved; a few are subrounded with a diameter of 3 mm. Note subcircular flat area (surrounded by yellow dashed line) without *Kinneyia*; around the flat area, crests and pits are fine-scaled and narrow, increasing in length and width outwards. Locality: Niederhagen Member, Farm Urikos (S 24◦.26_.56__, E 016◦.10_.56.6__). (H) Flat upper bedding surface of 15 cm thick quartzite bed with *Kinneyia* structure developed in an irregular patch with sharp margin. The margin of the patch is smooth and curved on the left side, but more irregular on the right side. The *Kinneyia* structure consists of crests and pits arranged mainly in a honeycomb-like pattern in the central part of the patch. Along the margin, pits and crests are much reduced in size. This is visible particularly along the left side of the patch; the crests and pits are fine-scaled and very narrow and seem aligned parallel to the margin. Locality: Vingerbreek Member, Farm Haruchas (S 24◦.21_.46.5__, E 016◦.24_.21.5__). Scale in cm. *Genesis of structures in Figures 7(h)-2F to -2H*: These examples illustrating '*Kinneyia* structures' show a diversity in shape and size, varying from simple, long, flat-topped crests covering large areas of a bedding surface to honeycomb-like arrangements of flat-topped crests and intervening elongate to round pits partly occurring as patches. Common features include the occurrence on flat bedding surfaces of sandstone layers and the occasional preservation of fine-grained sericitic material in the depressions. '*Kinneyia* structures' commonly occur on upper surfaces of sandy event beds, below fine-grained sericitic layers which may represent former microbial mat layers previously growing on the new sediment surface. *Kinneyia* structures are considered here as a category of 'subsurface structures' developed on flat sandy surfaces underneath mats (see Chapter 6(a)).

In: *Atlas of microbial mat features preserved within the clastic rock record*, Schieber, J., Bose, P.K., Eriksson, P.G., Banerjee, S., Sarkar, S., Altermann, W., and Catuneau, O., (Eds.)J. Schieber et al. (Eds.), Elsevier, p. 214-221. (2007)

Figure 7(h)-3: Mat destruction features: tepee-like shrinkage cracks in thin mat layers (A), curled shrinkage crack margins in thin mat layers (B–D), microbial shrinkage/sand cracks (E, F), upturned crack margins in biolaminites (G), polygonal pattern of upturned crack margins in biolaminites (H).
(A) Upper bedding surface of a biolaminite showing tepee-like structures. The structures are developed in a 2 mm thick layer and consist of isolated to bifurcating, straight to sinuous, upturned crack margins with inverted Vshaped cross-section, 2–3 mm high, and with tapering ends. In a few cases, the margins are gently overthrust and are organised as opposite/symmetric cracks (arrows). (B) Upper bedding surface of biolaminite showing narrow shrinkage cracks. The cracks are preserved either as imprints or narrow ridges on adjoining upper and lower surfaces of thin siltstone laminae within the biolaminites. The surface preserves isolated lenticular and curved cracks, subcircular cracks (upper right part of photo) and subrounded cracks with sinuous and irregular margins. Within one of the crack openings, millimetre-scale round-crested bulges forming a nodular structure (arrow) are preserved. (C) Close-up view of upper bedding surface in biolaminites showing imprints of simple isolated microbial shrinkage cracks and crack openings with subcircular to elongate irregular margins. Some of the crack openings preserve a millimetre-scale honeycomb-like reticulate pattern (arrow). (D) Upper bedding surface with incomplete network of microbial shrinkage cracks, partly arranged in a subcircular to elongate pattern. Green arrow indicates millimetre-scale round-crested bulges forming nodular structures in subcircular crack openings, similar to that of Figure 7(h)-3B. Note local development of isolated lenticular cracks (blue arrow). (E) Upper bedding surface of 3 cm thick fine-grained sandstone bed with microbial shrinkage cracks occurring as a single generation. The cracks form flattened ridges, randomly oriented and with lenticular, spindle or tri-radiate shape. They occur as isolated, straight to gently curved ridges, tapering at the ends. Locally the ridges are located along three opposite margins surrounding an opening in which a millimetre-scale reticulate pattern is preserved (arrow). (F) Upper bedding surface of 3 cm thick fine-grained quartzite layer with microbial shrinkage cracks preserved mainly as lenticular and partly as tri-radiate sandstone ridges. The cracks, tapering at the ends, merge together at high angles without cross-cutting relationships, and with a preferred orientation. (G) Section across a package of biolaminites showing 'upturned margin' structures (indicated by arrows). The cracks cut through multilayered biolaminite sections of variable thickness and their upturned margins form a symmetric inverted V-shaped structure. The structures are limited to thin packages of layers, usually less than 1 cm, which are upturned at an angle of 60–90∘. (H) Upper bedding surface of biolaminite preserving a polygonal network of subvertically upturned shrinkage crack margins. The upturned margins, 1–2 cm thick, form polygons of variable size and appear as sharp-crested folds or isolated belts of upturned lamination. *Genesis of structures in Figure 7(h)-3*: The shrinkage features presented in A to F illustrate the diversity in geometry and shape of structures related to subaerial desiccation of thin microbial mat layers. Similar structures occur in modern microbial mats that undergo shrinkage and cracking during subaerial exposure in the intertidal/lower supratidal zones of the southern Tunisian tidal flats (see Figure 4(c)-5D). The examples illustrate different stages of crack margin evolution and crack preservation. Tepee-like structures (Figure 7(h)-3A) develop in single and thin mat layers when crack margins are upturned without being completely detached from the sediment below, and without being involuted ('curled'). Such structures may be considered as the incipient stage within the evolution of shrinkage cracks in thin mat layers. When the crack margins evolve during progressive shrinkage, they may develop irregular to subcircular involute ridges surrounding the crack openings (Figures 7(h)-3B to -3D). Similarly, lenticular cracks may reflect an early stage of shrinkage without yet evolving to curled structures (Figures 7(h)-3C, -3D). The millimetre-scale bulges and reticulate patterns developed partly in the crack openings may reflect growth features of a new mat that grew on the exposed sediment surfaces. Preservation of such structures was favoured either by subsequent deposition of thin siltstone laminae or overgrowth of new mat layers. Cracks developed in thin microbial mat layers may be preserved as sand ridges by simple infillings of cracks by sand/silt sediment during subsequent tidal floods (Figures 7(h)-3E, -3F; see also Section 7(f)). Abundance of short lenticular and tri-radiate cracks indicates an incipient stage of shrinkage. Figure 7(h)-3F preserves also structures indicating curled margins (arrow) with millimetre-scale reticulate growth structure developed in the opening, similar to that of Figure 7(h)-3C. In contrast, subaerial desiccation of biolaminites and development of large and deep cracks involving thick 'multilayered' organo-sedimentary layers (biolaminites) produce structures of sub-vertically thin to thick upturned margins, which can form a wide polygonal network on bedding surfaces (Figures 7(h)-3G, -3H; see also Figure 4(c)-6). All shrinkage features illustrated here are developed during growth and accretion of biolaminite facies and record subaerial desiccation restricted to single microbial mat layers or encompassing thick biolaminite layers.
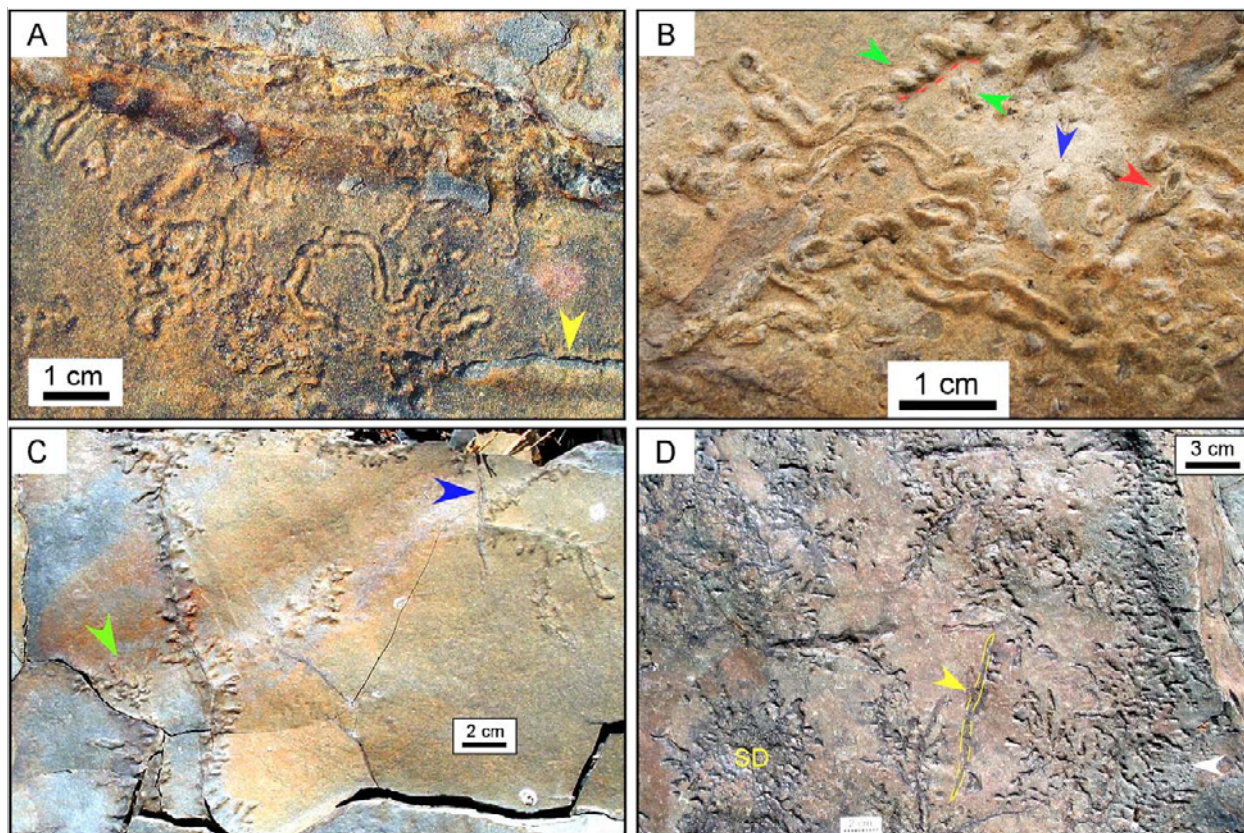
Figure 7(h)-4: Trace fossils/mat miners.
(A) Upper flat bedding surface of a 3 mm thick siltstone layer with straight to slightly irregular short tunnels, a few millimetres to less than 2 cm long, and simple meandering tunnels, ca. 6 cm long. Each trace fossil structure consists of an unbranched horizontal trail with a median groove flanked on both sides by ridges which usually have a curved termination at one end of the trace. Width of traces is uniform and ca. 2 mm. Arrow indicates associated spindle-shaped shrinkage crack. (B) Close-up view of upper bedding surface of a 4 mm thick siltstone layer with unbranched, sinuous to irregularly meandering and curved traces with a median furrow. The traces are 3 mm wide, 1–6 cm long, and flanked on both sides by round-crested ridges which usually join at one end of the trace. Some grooves preserve concentric curved lines (red arrow). Rarely, a median furrow (dashed line) is perpendicularly flanked on both sides by straight and elongate ridges (green arrows), 1–3 mm in length and about 1 mm wide. The ridges occur in positive relief and form spaced lateral bodies along the margin of a furrow or form isolated subrounded elements (blue arrow). (C) Upper bedding surface of millimetre-thick siltstone layer exhibiting straight to sinuous lines, from which straight to slightly curved irregular segments extend perpendicularly on both sides. The segments are 0.5 to 2 cm long and 1–2 mm wide, and are preserved in positive epirelief. Occasionally the segments form small isolated and irregular patches (green arrow). Blue arrow indicates associated lenticular shrinkage crack. (D) Upper bedding surface of a millimetre-thick siltstone layer with a high density of trace fossils in negative epirelief, consisting of up to 20 cm long, slightly curved furrows, from which straight to irregular troughs, 0.5–2 cm long, extend perpendicularly on both sides. In some cases, the central

furrows contain imprints or relics of sand-fillings of lenticular shrinkage cracks (yellow arrow). Occasionally, short troughs radiate from subcircular depressions (SD) or occur in irregular patches or as isolated features (white arrow). *Locality*: All photos from Vingerbreek member, Haruchas area. *Interpretation*: The trace fossils illustrated here form two distinct types (A–B and C–D) of bedding-parallel, horizontally oriented forms which may occur together on the same surfaces. The first type (A–B) is similar to traces which have been described from another section of the Vingerbreek member and referred to as *nereites and chondrites* by Crimes and Germs (1982). These trace fossils, also assigned to *Archaeonassa sp.* (Jensen, 2003; Jensen and Runnegar, 2005), are believed to reflect movement over a sandy surface at the sediment–water or sediment–air interface. The trace is also similar to that made by gastropods or mollusklike bilateral producers, left on wet sediment surfaces, by displacing sediment along the sides from the front into a terminal backfill (Jensen et al., 2005; Seilacher et al., 2005). The second type of trace fossils (C–D) are virtually identical to tunnel patterns of 'undermat miners', as documented by Seilacher (1999) from the Upper Cambrian of Oman. Seilacher (1999) noted the similarity of the traces to tunnel systems produced by bark beetles below modern mats which have become updomed. The position of the tunnels along shrinkage cracks seems to indicate that the miners use small crack openings in the mat surface to move underneath the mat. The cracks, moreover are sites of increased moisture and microbial activity. The trace fossils illustrated here have common features with the majority of trace fossils reported from Ediacaran strata (Hagadorn and Bottjer, 1999; Jensen et al., 2000, 2005; Seilacher et al., 2005): (i) they generally form simple and unbranched grazing trails; (ii) are essentially 'bed-parallel forms' indicating horizontally oriented behavioural activities, and (iii) are constructed close to the sediment surface or at the sediment–water interface. The two types of trace fossils are consistently bed-parallel forms, suggesting that the burrowing organisms were restricted to the uppermost, well oxygenated and microbially colonised sediment surface. This is also consistent with their association with microbial shrinkage cracks, developed in thin veneers of microbial mats. Also, preservation of such subtle structures would have been favoured by biostabilising microbes or covering microbial mats.

References

Aigner, T., and Reineck, H. E., 1982, Proximality trends in modern storm sands from the Helgoland Bight (North Sea) and their implications for basin analysis. Senckenbergiana Maritima 14, 183–215.

Crimes, T.P. and Germs, G.J.B., 1982, Trace fossils from the Nama Group (Precambrian-Cambrian) of Southwest Africa (Namibia). Journal of Paleontology 56, 890-907.

Gerdes G., and Klenke T., 2003, Geologiscje Bedeutung ökologischer Zeiträume in biogener Schichtung (Mikrobenmatten, potentielle Stromatolithe), Mitt. Ges. Geol. Bergbaustud. Österr., 46, 35-49.

Gerdes, G., Klenke, Th., and Noffke, N., 2000, Microbial signatures in peritidal siliciclastic sediments: A catalogue. Sedimentology 47, 279-308.

Germs, G.J.B., 1983, Implications of a sedimentary facies and depositional environmental analysis of the Nama Group in South West Africa/Namibia. Geological Society of South Africa, Special Publication 11, 89-114.

Germs, G.J.B., Knoll, A.H., and Vidal, G., 1986, Latest Proterozoic microfossils from the Nama Group, Namibia (South West Africa). Precambrian Research 32, 45-62.

Gresse, P.G., and Germs, G.J.B., 1993, The Nama foreland basin: sedimentation, major unconformity bounded sequences and multisided active margin advance. Precambrian Research 63, 247-272.

Grotzinger, J.P., Bowring, S.A., Saylor, B.Z. and Kaufman, A.J., 1995, New biostratigraphic and geochronologic constraints on early animal evolution. Science 270, 598-604.

Grotzinger, J.P., Watters, W.A. and Knoll, A.H., 2000, Calcified metazoans in thrombolite-stromatolite reefs of the terminal Proterozoic Nama Group, Namibia. Paleogeology 26, 334-359.

Hagadorn, J.W. and Bottjer, D.J., 1999, Restriction of a late Neoproterozoic biotope: suspect-microbial structures and trace fossils at the Vendian-Cambrian transition. Palaios, 14, 73-85.

Jensen. S., 2003, The Proterozoic and earliest Cambrian trace fossil record; patterns, problems and perspectives, Integrative and Comparative Biology, 43, 219-228.

Jensen, S., Saylor, B.Z., Gehling, J.G., and Germs, G.J.B., 2000, Complex

trace fossils from the terminal Proterozoic of Namibia, Geology, 28, 143-146.

Jensen, S., and Runnegar, B.N., 2005, A complex trace fossil from the Spitskop Member (terminal Ediacaran–? Lower Cambrian) of southern Namibia, Geological Magazine, 142, 561-569.

Jensen, S., Droser, M.L., and Gehling, J.G., 2005, Trace fossil preservation and the early evolution of animals, Pal. Pal. Pal., 220, 19-29.

Noffke, N., Knoll, A.H. and Grotzinger, J.P., 2002, Sedimentary controls on the formation and preservation of microbial mats in siliciclastic deposits: A case study from the Upper Neoproterozoic Nama Group, Namibia. Palaios 17, 533-544.

Porada, H., and Bouougri, E., 2006, Siliciclastic biolaminites and microbial mats structures in the Terminal Proterozoic Vingerbreek Member, Nama Group, Namibia, Sediment2006, Göttingen, Abstract, 136.

Saylor, B.Z., Grotzinger, J.P. and Germs, G.J.B., 1995, Sequence stratigraphy and sedimentology of the Neoproterozoic Kuibis and Schwarzrand subgroups (Nama Group), southwestern Namibia. Precambrian Research 73, 153-172.

Seilacher, A., 1999, Biomat-related lifestyles in the Precambrian. Palaios 14, 86-93.

Seilacher, A., Buatois, L.A., Mángano M.G., 2005, Trace fossils in the Ediacaran-Cambrian transition: Behavioral diversification, ecological turnover and environmental shift, Pal. Pal. Pal., 227, 323-356.